The Canadian Mineralogist
Vol. 38, pp. 57-65 (2000)

ZIRCONOLITE WITH SIGNIFICANT *REE*ZrNb(Mn,Fe)O_7 FROM A XENOLITH OF THE LAACHER SEE ERUPTIVE CENTER, EIFEL VOLCANIC REGION, GERMANY

GIANCARLO DELLA VENTURA§

Dipartimento di Scienze della Terra, Università della Calabria, I-87036 Arcavacata di Rende (CS), Italy

FABIO BELLATRECCIA

Museo di Mineralogia, Università di Roma La Sapienza, P. Aldo Moro 5, I-00185 Roma, Italy

C. TERRY WILLIAMS

Department of Mineralogy, The Natural History Museum, Cromwell Road, London SW7 5BD, U.K.

Abstract

We report a new occurrence of the mineral zirconolite, ideally $CaZrTi_2O_7$, from xenoliths in the pyroclastic formations outcropping near Niedermendig, Laacher See eruptive center, Eifel volcanic region, Germany. This example of zirconolite is crystalline, a rare feature for a mineral of this group; it gives an X-ray-diffraction pattern corresponding to the orthorhombic polytype (zirconolite-3*O*), space group *Acam*, with *a* 10.145(8), *b* 14.18(8), *c* 7.284(5) Å. It contains the highest concentration of Mn reported from natural zirconolite (6% MnO); it is also rich in Nb (~18% Nb_2O_5) and *REE* (up to 19.4% Y_2O_3 + REE_2O_3), with Ce the dominant *REE*. The mineral formula, expressed in terms of three of the five end-member components identified for the compositional space of zirconolite, is: 32% $CaZrTi_2O_7$, 53% *REE*Zr*Me*$^{5+}$*Me*$^{2+}O_7$, and 6% *ACT*ZrTi*Me*$^{2+}O_7$ (with 9% unassigned). The compositional variation can best be described by the coupled substitution: REE^{3+} + (Fe^{2+},Mn^{2+}) + Nb^{5+} ↔ Ca + 2Ti. The host rock is an alkali syenite xenolith almost exclusively composed of alkali feldspar ($Or_{45}Ab_{55}$), with minor biotite. Zirconolite crystallizes as an accessory mineral in voids between feldspar crystals, together with baddeleyite, manganoan magnetite, and monazite-(La), a rare species of monazite. This suite of minerals, with their unusual chemical compositions, crystallized from late-stage metasomatic fluids enriched in Nb and Mn, and having an exceptional La-enriched *REE* signature.

Keywords: zirconolite, unit-cell parameters, crystal chemistry, monazite-(La), Laacher See eruptive center, Eifel volcanic region, Germany.

Sommaire

Nous décrivons un nouvel exemple de zirconolite, de composition idéale $CaZrTi_2O_7$, provenant de xénolithes récupérés d'une séquence pyroclastique près de Niedermendig, et faisant partie du centre éruptif de Laacher See, région volcanique d'Eifel, en Allemagne. Fait important à signaler, cet exemple de zirconolite est cristallin; le spectre de diffraction X correspond au polytype orthorhombique (zirconolite-3*O*), groupe spatial *Acam*, *a* 10.145(8), *b* 14.18(8), *c* 7.284(5) Å. Sa teneur en Mn est la plus élevée qui ait été signalée (6% MnO); il est aussi enrichi en Nb (~18% Nb_2O_5) et en terres rares, *TR* (jusqu'à 19.4% de Y_2O_3 + TR_2O_3), le Ce surtout. Sa formule chimique, exprimée ici en termes de trois des cinq composantes nécessaires pour définir le champ de composition de la zirconolite, est: 32% $CaZrTi_2O_7$, 53% *TR*Zr*Me*$^{5+}$*Me*$^{2+}O_7$, et 6% *ACT*ZrTi*Me*$^{2+}O_7$ (avec 9% non assigné). La composition varie surtout selon la substitution couplée TR^{3+} + (Fe^{2+},Mn^{2+}) + Nb^{5+} ↔ Ca + 2Ti. La roche hôte est une syénite alcaline contenant presqu'exclusivement un feldpath alcalin ($Or_{45}Ab_{55}$), avec biotite accessoire. La zirconolite cristallise dans les espaces entre les cristaux de feldspath, avec baddeleyite, magnétite manganifère, et la monazite-(La), membre rare du groupe de la monazite. Cette suite de minéraux, avec une composition chimique inhabituelle, a cristallisé à partir de fluides tardifs d'origine métasomatique, enrichis en Nb et Mn, avec un enrichissement exceptionnel en La parmi les terres rares.

(Traduit par la Rédaction)

Mots-clés: zirconolite, paramètres réticulaires, chimie cristalline, monazite-(La), centre éruptif de Laacher See, région volcanique d'Eifel, Allemagne.

§ *E-mail address*: dellaven@unical.it

Introduction

Zirconolite is a relatively rare accessory mineral, ideally $CaZrTi_2O_7$ in composition, but generally accommodating a large number of elements in its structure. With its extensive substitutions, it may be best described in terms of five hypothetical end-member components (Gieré *et al.* 1998), listed below. In addition to having a large compositional range, zirconolite also exists as several polytypes (Bayliss *et al.* 1989, Smith & Lumpkin 1993). However, as it can incorporate significant amounts of actinide elements (Th and U) into its structure, zirconolite in the majority of cases is partially or completely metamict, and its structure cannot be resolved easily. Here, the young age of the Eifel volcanic complex, coupled with the relatively low content of actinide elements (*ACT*) in zirconolite, combine to allow retention of much of the original crystal structure and enable a single-crystal X-ray pattern to be obtained, and the structure to be determined.

Although zirconolite occurs in a wide range of rock types (*e.g.*, Williams & Gieré 1996), it has only rarely been reported from syenites. In this study, we describe the crystallography and unusual composition of zirconolite and its coexistence with the rare monazite species monazite-(La) within the late-stage alteration of a syenitic ejectum enclosed in the pyroclastic successions of the Laacher See volcanic center, Eifel volcanic region, Germany. This report contributes further to our knowledge of the complex mineralogy and chemical composition of zirconolite, and in particular, to its crystallization from a fluid exceptionally enriched in light rare-earth elements (*REE*) and Mn.

Background Information on the Crystallography and Crystal Chemistry of Zirconolite

Zirconolite, ideally $CaZrTi_2O_7$, has five cation-acceptor sites: Ca in 8-coordination (*M*8 site), Zr in 7-coordination (*M*7), three distinct Ti sites, (*M*6) in 6-coordination, and a pair of 5-coordinated *M*5 sites (*e.g.*, Gieré *et al.* 1998). The large variation in polyhedral volumes of these sites, ranging from 5.7 $Å^3$ for the *M*5 site to 21.3 $Å^3$ for the *M*8 site (Fielding & White 1987), provides a structure capable of accommodating many elements, and in natural samples of zirconolite, thirty or more elements may be present at the 0.1 to 1.0 wt% concentration level (*e.g.*, Williams & Gieré 1996). Substituting cations range in size (ionic radii data from Shannon 1976) from 0.051 (Ti^{4+}) to 0.112 nm (Ca^{2+}), and charge from 2+ (Mg) to 6+ (W). The principal substitutions are: the rare-earth elements and actinide elements for Ca, Hf for Zr, and Nb, Ta, Fe, Mn, Mg and W for Ti. On the basis of observations made on naturally occurring and synthetic zirconolite, Gieré *et al.* (1998) identified five hypothetical end-members, these being $CaZrTi_2O_7$, $CaZrMe^{5+}Me^{3+}O_7$, $ACTZrTiMe^{2+}O_7$, $REEZrTiMe^{3+}O_7$ and $REEZrMe^{5+}Me^{2+}O_7$. Within this multicomponent system, twenty-four possible substitutions have been identified, of which only five or six are important in natural samples (Gieré *et al.* 1998).

In natural samples, three polytypes of zirconolite have been reported: zirconolite-2*M* is the two-layered monoclinic aristotype (see White 1984), zirconolite-3*T* is the three-layered trigonal polytype, and zirconolite-3*O* is the three-layered orthorhombic polytype (Mazzi & Munno 1983, Bayliss *et al.* 1989). In synthetic samples, two additional polytypes, zirconolite-4*M* and zirconolite-6*T*, have been identified (Smith & Lumpkin 1993, Coelho *et al.* 1997), and described as supercells of the corresponding monoclinic and trigonal phases. The Bayliss *et al.* (1989) IMA-approved scheme of nomenclature stipulates that the name zirconolite should be employed for the non-crystalline (metamict) mineral, or for an undetermined naturally occurring polytype of $CaZrTi_2O_7$. Of the many reported natural occurrences of zirconolite, in only a few can the structure be confidently assigned, or reliably inferred. These are from Cape Verde (Silva & Figueiredo 1980), Campi Flegrei (Mazzi & Munno 1983), Kaiserstuhl (Sinclair & Eggleton 1982), Sebl'yavr (Bulakh *et al.* 1998), Jacupiranga (Sinclair & Ringwood 1981), Bergell (Lumpkin *et al.* 1997) and several from Kola Peninsula (G.R. Lumpkin, pers. commun. 1999).

Although zirconolite occurs in a wide range of rock types and parageneses, the majority from carbonatites (Gieré *et al.* 1998), it has been reported from only four syenite occurrences out of a total of more than 50 terrestrial localities (Williams & Gieré 1996): (1) at Glen Dessarry, Scotland (*e.g.*, Fowler & Williams 1986), as very small grains (typically <10 μm) enclosed in alkali feldspar phenocrysts, (2) from the alkali intrusion of the Arbarastakh Massif, Russia (Borodin *et al.* 1960), (3) in syenite pegmatites in the Oslo region of Norway at Fredicksvärn (Brøgger 1890) and Langesundfjord (Larsen 1996), and (4) from a syenitic ejectum enclosed in the explosive volcanic deposits at Campi Flegrei, Italy (Mazzi & Munno 1983).

Analytical Techniques Employed

To augment standard optical microscopic techniques, petrological and chemical information at high resolution was obtained using a Philips XL30 scanning electron microscope (SEM) coupled with an EDAX energy-dispersion system of analysis. The SEM was operated at an accelerating voltage of 25 kV and a beam current of 0.3 nA at LIME (Laboratorio di Microscopia Elettronica, Università di Roma Tre, Italy). Quantitative chemical analyses of the mineral phases were obtained with a Cameca SX–50 wavelength-dispersion electron microprobe (at the Natural History Museum, London, U.K.) operated at an accelerating voltage of 20 kV and a beam current of 20 nA. A spot size of 5 μm was used for mica and feldspar, whereas a spot size of 1 μm was used for all other minerals. The small size of

the zirconolite and baddeleyite grains analyzed introduces the possibility of fluorescence effects from adjacent phases and consequently some analytical error. However, the absence of significant Si and Al suggests that this effect was negligible, since these elements are the most probable "contaminants" from the feldspar matrix. Characteristic X-ray lines of all the elements sought, background positions employed and standards used are presented in Table 1. Inter-element interferences, particularly for the rare-earth elements, were based on the procedure given in Williams (1996), and were corrected empirically in this study.

The X-ray-diffraction pattern of zirconolite (Cu*K*α, Ni-filtered radiation at 40 kV, 20 mA, 48 hours exposure) was obtained from a single crystal mounted in a Gandolfi camera (114 mm radius).

Petrography and Mineral Compositions

The zirconolite- and monazite-bearing specimen described here is a small (3 to 4 cm diameter) fragment of fine-grained syenite collected from the pyroclastic sequence belonging to the late Quaternary Laacher See eruptive center, outcropping near Niedermendig, Germany. Explosive eruptions of the Laacher See volcano (~11,000 years old) produced fallout and surge deposits more than 50 m thick near the vent (Bogaard & Schmincke 1984). These pyroclastic rocks are locally enriched in xenoliths of various types, including regional metamorphic and contact metamorphic rocks (*e.g.*, hornfels, spotted mica schists: Wörner *et al.* 1982). The sample studied here has a porphyritic texture consisting of elongate and intergrown perthitic alkali feldspar phenocrysts**.** The phenocrysts generally display Carlsbad twinning, they are inclusion-rich and are compositionally homogeneous, corresponding approximately to $Or_{44}Ab_{55}An_{01}$ (Table 2). Of the minor elements sought using the microprobe, neither Sr nor Ba were detected.

The interlocking nature of the feldspar crystals gives rise to small (millimeter-size) miarolitic cavities that host the assemblage of accessory minerals: biotite, magnetite, monazite, baddeleyite and zirconolite. The biotite has a Mg/(Mg + Fe) ratio around 0.55 and thus is ferroan phlogopite; it has a high Mn content (average MnO ≈ 5.3%, Table 2). Magnetite forms typically roundish, subhedral crystals and also is rich in both Mn and Ti, corresponding to approximately $Mgt_{80}Gal_{20}$ (Table 2). Some of the magnetite crystals show evidence of later intensive corrosion and alteration to produce a skeletal "residue" of iron oxides that is depleted in both Mn and Ti.

TABLE 1. ANALYTICAL DETAILS USED IN THE ELECTRON-MICROPROBE ANALYSES OF ZIRCONOLITE

Element	Standard used	Line	Peak position (sinΘ)*10⁵	Background position(s) relative to peak positive	Background position(s) relative to peak negative	Interfering elements corrected for
Mg	periclase	*K*α	38499	-	800	-
Al	corundum	*K*α	32463	600	-	-
Si	wollastonite	*K*α	27737	600	-	-
Ca	perovskite*	*K*α	38387	500	-	-
Ti	perovskite*	*K*α	31416	500	-	-
Mn	pure Mn***	*K*α	52200	3450	500	-
Fe	pure Fe***	*K*α	48083	3618	2682	-
Y	Y glass**	*L*α	73710	-	1310	-
Zr	ZrO_2*	*L*α	69386	600	-	-
Nb	$NaNbO_3$*	*L*α	65429	500	-	-
La	La glass**	*L*α	30469	265	695	-
Ce	Ce glass**	*L*α	26931	496	-	Ti
Pr	Pr glass**	*L*β	56098	8651	449	-
Nd	Nd glass**	*L*α	58870	5880	3220	Ce
Sm	Sm glass**	*L*α	54633	1016	2935	Ce
Gd	Gd glass**	*L*α	50833	866	5434	Ce, La
Dy	Dy glass**	*L*α	47406	4293	2007	Mn, Fe, Th
Er	Er glass**	*L*α	44313	1087	5813	Fe
Hf	pure Hf***	*L*α	38981	500	-	-
Ta	pure Ta***	*L*α	37799	500	-	-
Pb	galena	*M*α	60420		1000	Nb
Th	pure Th***	*M*α	47299	500	-	-
U	UO_2*	*M*β	42474	500	-	-

* synthetic oxides; ** individual *REE*–Ca–Al silicate glasses. *** pure metals. All other standards are well-characterized natural minerals.

TABLE 2. ELECTRON-MICROPROBE DATA FOR ALKALI FELDSPAR, MICA AND SPINEL FROM LAACHER SEE XENOLITH

	Alkali feldspar Mean (6)	σ		Mica Mean (10)	σ		Magnetite Mean (7)	σ
SiO_2 wt%	65.6	0.5		36.0	0.6		0.07	0.07
TiO_2	0.03	0.02		2.56	0.23		6.1	0.2
Al_2O_3	19.2	0.2		13.4	0.3		1.56	0.04
Cr_2O_3	-	-		0.03	0.02		0.03	0.02
Fe_2O_3**	0.15	0.04		-	-	Fe_2O_3***	54.3	-
FeO	-	-		16.3	0.3	FeO***	25.5	-
Nb_2O_5	-	-		-	-		0.06	0.05
CaO	0.21	0.07		<0.02	-		<0.02	-
MgO	<0.02	-		11.1	0.4		0.30	0.03
MnO	<0.02	-		5.28	0.11		10.7	0.2
BaO	<0.05	-		0.04	0.03		-	-
Na_2O	6.6	0.31		0.57	0.03		-	-
K_2O	7.9	0.48		9.3	0.13		-	-
Total	99.7			94.6			98.6	
Basis	8 oxygen atoms			22 oxygen atoms			4 oxygen atoms	
Si *apfu*	11.86	0.02		5.62	0.04		0.02	0.02
Ti	0.00	0.00		0.30	0.03		1.41	0.05
Al	4.09	0.02		2.47	0.06		0.57	0.02
Cr	-	-		0.00	0.00		0.01	0.01
Fe^{3+}	0.02	0.01		-	-		12.53	0.12
Fe^{2+}	-	-		2.14	0.06		6.54	0.03
Mn	-	-		0.70	0.02		2.78	0.05
Mg	-	-		2.59	0.07		0.14	0.01
Ca	0.04	0.01		0.00	0.00		0.01	0.00
Ba	-	-		0.00	0.00		-	-
Na	2.30	0.11		0.17	0.01		-	-
K	1.82	0.02		1.85	0.01		-	-
Σcations	20.13			15.85			23.99	
Ab	55.4	2.40	mg*	0.54	0.01	Fe_3O_4	0.81	
An	1.0	0.30				$MgFe_2O_4$	0.01	
Or	43.7	2.70				$MnTiO_4$	0.18	

* Mg/(Mg + Fe); ** All Fe as Fe_2O_3; *** FeO/Fe_2O_3 calculated according to Droop (1987). σ: standard deviation.

Baddeleyite is rare, forms small crystals (<10 μm), and is usually found in association (in some cases intergrown) with zirconolite within the cavities and fractures among the feldspar crystals (Fig. 1). Baddeleyite generally has a composition close to stoichiometric ZrO_2, with published analyses typically showing only Hf (and, more rarely, Nb) at concentrations >1% (*e.g.*, Heaman & LeCheminant 1993). Baddeleyite from Laacher See contains significant amounts of Hf, Ti, Fe and Nb (Table 3).

Monazite-(La)

Monazite-(La) typically occurs as well-developed subhedral to euhedral crystals, up to 50 μm in diameter, in the angular miarolitic cavities among feldspar grains. Monazite is homogeneous in composition and close to ideal *REE*(PO_4), with only a limited incorporation of Si, Th and Ca. The average result of nine electron-microprobe analyses is given in Table 3; La is the dominant *REE*, confirming that the mineral is the relatively uncommon species monazite-(La). The vast majority of examples of monazite reported in the literature are monazite-(Ce), with monazite-(La) and monazite-(Nd) only rarely encountered (Chang *et al*. 1996).

TABLE 3. ELECTRON-MICROPROBE DATA FOR MONAZITE-(La) AND BADDELEYITE FROM LAACHER SEE XENOLITH

	Monazite Mean (9)	σ		Baddeleyite Mean (5)	σ
SiO_2 wt%	0.82	0.18	MgO	<0.02	-
P_2O_5	29.5	0.3	Al_2O_3	0.18	0.35
CaO	0.13	0.03	SiO_2	0.45	1.00
Fe_2O_3	0.02	0.02	CaO	0.04	0.02
Y_2O_3	0.09	0.07	TiO_2	0.41	0.18
La_2O_3	35.7	1.1	Cr_2O_3	0.03	0.03
Ce_2O_3	29.2	0.7	MnO	0.26	0.11
Pr_2O_3	1.21	0.13	FeO	0.60	0.49
Nd_2O_3	2.03	0.32	ZrO_2	94.3	1.5
Sm_2O_3	0.30	0.04	Nb_2O_5	2.2	0.85
Eu_2O_3	<0.15	-	HfO_2	1.40	0.11
Gd_2O_3	<0.10	-	Total	99.8	
Dy_2O_3	<0.07	-			
Er_2O_3	<0.07	-			
ThO_2	1.58	0.32			
UO_2	0.05	0.04			
Total	100.6				
Basis	4 atoms of oxygen			2 atoms of oxygen	
Si *apfu*	0.032	0.007	Al *apfu*	0.004	0.008
P	0.972	0.007	Si	0.009	0.020
S (P + Si)	1.004	0.002	Ca	0.001	0.000
			Ti	0.006	0.003
Ca	0.005	0.001	Cr	0.000	0.000
Fe	0.000	0.001	Mn	0.005	0.002
Y	0.002	0.001	Fe	0.010	0.009
La	0.512	0.017	Zr	0.940	0.022
Ce	0.416	0.009	Nb	0.020	0.008
Pr	0.017	0.002	Hf	0.008	0.001
Nd	0.028	0.004	Σcations	1.004	0.000
Sm	0.004	0.001			
Th	0.014	0.003			
U	0.000	0.000			
Σ*A*	0.999	0.005			
Σcations	1.997	0.000			

σ: standard deviation.

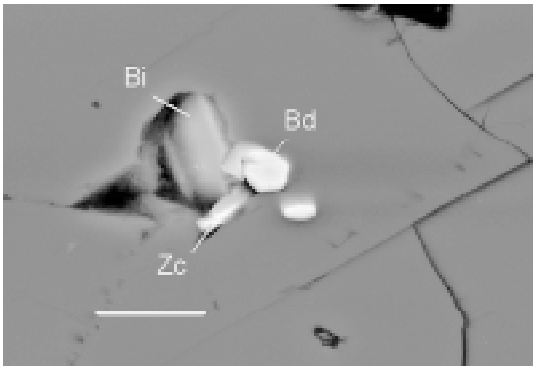

FIG. 1. Back-scattered electron image of baddeleyite (Bd) associated with zirconolite (Zc) and biotite (Bi) in a small cavity between intersecting crystals of alkali feldspar (dark grey). The scale bar is 10 μm.

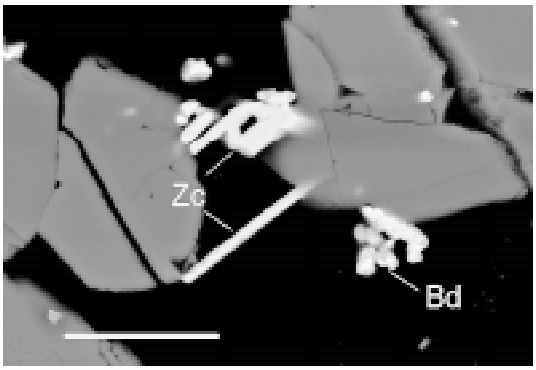

FIG. 2. Back-scattered electron image of acicular zirconolite (Zc) in a miarolitic cavity between crystals of alkali feldspar (dark grey). The scale bar is 20 μm.

Zirconolite

Zirconolite occurs as very rare, small, usually acicular crystals (maximum length ~5–10 μm) located in the cavities and fractures of feldspar (Fig. 2). It is transparent, with reddish brown color when viewed in transmitted light under an optical microscope.

X-ray diffraction

A single, small, acicular crystal of zirconolite (~20 μm in length and 2–3 μm in diameter) was removed from a vug in the rock. Its X-ray-diffraction pattern dis-

TABLE 4. X-RAY POWDER-DIFFRACTION PATTERN OF ZIRCONOLITE FROM LAACHER SEE, GERMANY

h k l	*d* (Å)	I	Refined unit-cell parameters	
2 0 2	2.96	m	*a* (Å)	10.145(8)
2 4 0	2.90	s	*b* (Å)	14.18(2)
0 4 2	2.54	w	*c* (Å)	7.284(5)
4 4 2	1.79	w	*V* (Å³)	1048.2
0 8 0	1.77	vw	space group	*Acam*
2 4 4	1.54	vw		
2 8 2	1.52	vw		

Intensities visually estimated: s: strong, m: medium, w: weak, vw: very weak.

plays only a few lines, but all are sharp (Table 4), establishing the crystal to be non-metamict, unlike the majority of natural crystals of zirconolite reported in the literature. The pattern corresponds well with that of zirconolite-3*O* by Mazzi & Munno (1983), and was indexed in the orthorhombic space-group *Acam*. Refined unit-cell parameters are given in Table 4.

As outlined above, zirconolite exists in many polytypes, and has a wide compositional range. In laboratory experiments, only the aristotype structure zirconolite-2*M* and its polytype (zirconolite-4*M*) have been synthesized (Smith & Lumpkin 1993, Coelho *et al*. 1997), where a transition from 2*M* to 4*M* occurs with an increasing proportion of Nd in the structure. Zirconolite-3*T* also has been synthesized, but only within a very narrow range of incorporated Nd (Coelho 1995). However, in natural samples, it is not known whether the chemical composition and the paragenesis influence its structural polytype, as the presence of even minor amounts of actinide elements usually renders the mineral at least partially metamict and therefore not amenable to resolution of the very minor structural differences that exist among the various polytypes. Of the many reported occurrences of zirconolite (>50), in only a few cases can the structure be confidently assigned, or reliably inferred. However, what scarce evidence exists indicates that zirconolite from carbonatitic environments forms either monoclinic zirconolite-2*M* or cubic zirkelite. Orthorhombic zirconolite-3*O* described here and zirconolite-3*T* and -3*O* from Campi Flegrei (Mazzi & Munno 1983) are from metasomatic environments associated with syenitic intrusions. The compositional data from Mazzi & Munno (1983) are unfortunately incomplete as the published analytical total is <80% (with concentrations of Mn, Nb and *REE* not established), and no material is available for further investigation (R. Munno, pers. commun., 1992). There are also some significant differences in zirconolite composition that correlate with paragenesis (Gieré *et al*. 1998), but as yet there are too few data to link these compositional differences with structural type. Clearly, further new studies of non-metamict zirconolite are needed to test this tentative correlation of structural type with paragenesis or mineral chemistry (or both).

Chemical composition

Several of the larger grains (typically 5–10 μm in size) were analyzed, and the data are given in Table 5. From these data, it is apparent that zirconolite is homogeneous, this being verified by back-scattered electron images; the zoning commonly observed in zirconolite is absent (*e.g.*, Williams & Gieré 1988, 1996, Bellatreccia *et al*. 1999). The concentrations of the major constituents (*i.e.*, Ca, Ti and Zr) are among the lowest so far recorded from terrestrial environments. To compensate for these low values, the Laacher See zirconolite is enriched in Fe and Nb relative to the mean of zirconolite values from Williams & Gieré (1996), and in addition has exceptionally high concentration levels of Mn and *REE*. The Mn content of the Laacher See zirconolite is particularly noteworthy (MnO = 6.0%). Although synthetic zirconolite has been doped with Mn at levels >5 wt% MnO (Kesson *et al*. 1983), Mn is usually only a minor constituent in natural terrestrial zirconolite, [average = 0.33% MnO, Williams & Gieré (1996), with a maximum value of 2.0% (Zakrzewski *et al*. 1992)]. In addition, the *REE* concentration of 19.4% is one of the highest recorded for natural, terrestrial zirconolite (the maximum being 23.7%: Fowler & Williams 1986).

Chemical substitutions

In the zirconolite from Laacher See, the [8]-coordinated Ca-site (*A* site, or *M*8 site according to the nomenclature of Mazzi & Munno 1983) is occupied by almost 60% *REE* plus minor amounts of Th + U (Table 5). The [7]-coordinated *B* site (*M*7) is occupied by Zr plus Hf. The three *C* sites (two *M*6 octahedra and one [5]-coordinated polyhedron, *M*5) are predominantly occupied by Ti, but there is an extensive incorporation of Fe, Mn and, notably, Nb. Although the sum of all the cations amounts to 3.996, *i.e.*, close to the ideal value of 4.00 (based on seven atoms of oxygen), the *A* and *B* sites are only approximately 90% filled, whereas the sum of the *C* sites are overfilled by approximately 20%. To balance this discrepancy in the site occupancy, we suggest that some of the Mn resides in both *A* and *B* sites. The ionic radius of 7- and 8-coordinated Mn^{2+} is 0.090 nm and 0.096 nm, respectively (Shannon 1976), which compares with 0.078 nm for Zr^{4+} and 0.112 nm for Ca^{2+}. Incorporation of Mn^{2+} into the Ca site has been inferred to occur in some cases of natural zirconolite (Gieré *et al.* 1998) and has been observed also in synthetic zirconolite (Kesson *et al*. 1983).

Of the five hypothetical end-members that constrain the composition of zirconolite (Gieré *et al*. 1998, Fig. 3), the sample from Laacher See can be expressed within the plane defined by three of these; it has a formula corresponding to: 32% $CaTiZr_2O_7$, 53% *REE*Zr*Me*$^{5+}$ *Me*$^{2+}O_7$, and 6% *ACT*Zr*Me*$^{2+}O_7$. Full correspondence is not achieved because of the apparent deviation from

stoichiometry ($\Sigma A \approx 0.9$, $\Sigma B \approx 0.9$ and $\Sigma C \approx 2.2$, Table 5). Thus approximately 9% cannot be assigned to any of the remaining two hypothetical end-members, as Zr is fully accounted for within this calculation, unless some of the excess cations (mainly Ti, Me^{2+} and Me^{5+}) substitute for Zr. Both a slight deficit and an excess in *B*-site totals have been reported for natural zirconolite (Gieré *et al*. 1998), suggesting the possibility of substitution at this site.

TABLE 5. SELECTED ELECTRON-MICROPROBE DATA FOR ZIRCONOLITE FROM LAACHER SEE XENOLITH

	1	2	3	4	5	Mean (5)	σ
MgO wt%	0.05	0.03	0.03	0.03	0.03	0.03	0.01
Al_2O_3	0.29	0.24	0.25	0.24	0.28	0.26	0.03
SiO_2	0.17	0.02	0.08	0.00	0.06	0.07	0.06
CaO	4.08	4.06	4.27	4.06	4.38	4.17	0.14
TiO_2	15.74	16.42	15.51	16.24	15.90	16.0	0.37
MnO	5.92	6.52	5.81	6.08	5.67	6.0	0.33
FeO	5.40	5.01	5.64	5.35	5.43	5.4	0.23
Y_2O_3	2.14	2.22	2.07	2.44	2.11	2.20	0.15
ZrO_2	25.40	25.87	25.29	25.84	25.95	25.7	0.30
Nb_2O_5	18.17	17.77	18.83	17.75	18.04	18.1	0.44
La_2O_3	3.23	3.06	2.78	2.62	3.00	2.94	0.24
Ce_2O_3	11.18	10.98	9.57	9.29	10.20	10.2	0.83
Pr_2O_3	1.07	0.98	0.90	0.76	0.94	0.93	0.11
Nd_2O_3	2.39	2.38	2.13	2.03	2.22	2.23	0.16
Sm_2O_3	0.20	0.23	0.16	0.21	0.21	0.20	0.03
Gd_2O_3	0.20	0.24	0.20	0.27	0.24	0.23	0.03
Dy_2O_3	0.14	0.15	0.24	0.26	0.21	0.20	0.05
Er_2O_3	0.19	0.12	0.19	0.22	0.18	0.18	0.04
HfO_2	0.32	0.29	0.30	0.31	0.45	0.33	0.07
Ta_2O_5	0.38	0.39	0.39	0.46	0.36	0.40	0.04
PbO	<0.1	<0.1	<0.1	<0.1	<0.1	<0.1	-
ThO_2	1.31	0.83	3.71	4.48	2.63	2.6	1.55
UO_2	0.53	0.57	1.21	1.36	0.67	0.9	0.39
Total	98.5	98.4	99.5	100.3	99.1	99.2	0.8
$Y+REE_2O_3$	20.7	20.4	18.2	18.1	19.3	19.3	1.2
Basis of 7 atoms of oxygen							
Ca *apfu*	0.316	0.313	0.329	0.312	0.337	0.321	0.011
Y	0.082	0.085	0.079	0.093	0.081	0.084	0.005
La	0.086	0.081	0.074	0.069	0.080	0.078	0.007
Ce	0.296	0.289	0.252	0.244	0.269	0.270	0.023
Pr	0.028	0.026	0.023	0.020	0.025	0.024	0.003
Nd	0.062	0.061	0.055	0.052	0.057	0.057	0.004
Sm	0.005	0.006	0.004	0.005	0.005	0.005	0.001
Gd	0.005	0.006	0.005	0.006	0.006	0.005	0.001
Dy	0.003	0.003	0.006	0.006	0.005	0.005	0.001
Er	0.004	0.003	0.004	0.005	0.004	0.004	0.001
Pb	0.000	0.000	0.000	0.000	0.000	0.000	0.000
Th	0.022	0.014	0.061	0.073	0.043	0.042	0.025
U	0.008	0.009	0.019	0.022	0.011	0.014	0.006
ΣA	0.917	0.895	0.912	0.907	0.921	0.910	0.010
Zr	0.894	0.907	0.888	0.902	0.910	0.900	0.009
Hf	0.007	0.006	0.006	0.006	0.009	0.007	0.001
ΣB	0.901	0.913	0.894	0.909	0.919	0.907	0.010
Ti	0.855	0.888	0.840	0.875	0.860	0.864	0.019
Si	0.012	0.002	0.005	0.000	0.004	0.005	0.005
Mg	0.005	0.003	0.003	0.004	0.003	0.004	0.001
Mn	0.362	0.397	0.354	0.369	0.345	0.366	0.020
Fe	0.326	0.301	0.339	0.320	0.326	0.323	0.014
Al	0.025	0.021	0.021	0.020	0.024	0.022	0.002
Nb	0.593	0.578	0.613	0.575	0.586	0.589	0.015
Ta	0.008	0.008	0.008	0.009	0.007	0.008	0.001
ΣC	2.186	2.197	2.183	2.171	2.156	2.179	0.016
Σcations	4.004	4.006	3.989	3.986	3.996	3.996	0.009
$\Sigma(Y+REE)$	0.571	0.560	0.502	0.500	0.530	0.533	0.029

σ: standard deviation.

Of the many substitutions possible in the zirconolite structure, only a few are geologically relevant. Several of the proposed substitutions describe the incorporation of *REE* at the *M*8 site (Gieré *et al*. 1998), and each can operate in different geological environments. Although the oxidation–reduction reactions of the crystallizing environment are difficult to assess, there is evidence to suggest that the redox conditions prevailing at the time of the zirconolite formation may exert some control on the mechanisms of substitution involved, and on the total amounts of *REE* and actinides accommodated by the structure (Gieré *et al*. 1998). Statistical analysis of a large number of chemical data of zirconolite from carbonatitic rocks suggests that in environments where both *REE* and pentavalent cations (Me^{5+} = Nb + Ta) are relatively abundant, incorporation of *REE* occurs mainly *via* the *REE* + Ti ↔ Ca + Me^{5+} substitution (#22, Gieré *et al*. 1998). However, as can be seen from the compositional-space diagram for natural zirconolite (Gieré *et al*. 1998, Fig. 3), this substitution cannot operate initially from the ideal zirconolite formula, but first requires substitution of *REE* or Me^{5+} (or both) in an initial exchange such as in substitutions #2 or #20 given by Gieré *et al*. (1998). Iron can exist as either divalent or trivalent cations, and for *REE*-enriched zirconolite (*i.e.*, $\Sigma Y + REE > 0.12$ *apfu*), particularly from carbonatites, the coupled substitution *REE* + Me^{3+} ↔ Ca + Ti (#20, Gieré *et al*. 1998) involving trivalent cations (Me^{3+} = Al + Fe) can be significant, provided oxidizing conditions exist. In zirconolite from Laacher See, the Σ(Mn + Fe) almost equals that of $\Sigma(Nb + Ta)^{5+}$ (Table 5), suggesting that substitution #21 of Gieré *et al.* (1998), *i.e.*, *REE* + Me^{2+} + Me^{5+} ↔ Ca + 2Ti, is the most important in controlling the chemical composition of this sample (where here, Me^{2+} = Fe, Mn). This substitution is shown in Figure 3, in which the data from the Laacher See sample are plotted together with data from high-*REE* zirconolite from Adamello (Gieré & Williams 1992). The good correlation suggests that both Fe (and Mn) indeed occur mainly in their divalent state, as also documented for the Adamello high-*REE* zirconolite (Gieré 1990, Gieré & Williams 1992). However, for the Laacher See sample, the redox conditions are more difficult to constrain; although some zirconolite crystals are associated with (and in some cases included within) larger crystals of magnetite, the large stability-field of magnetite does not allow for an accurate prediction of the redox conditions.

REE patterns

Because of its compliant structure, zirconolite does not appear preferentially to host the various *REE*, with the exceptions of La and Ce (Gieré 1986, Williams & Gieré 1988). This is because the 8-coordinated *A* site, which the *REE* predominantly occupy, does not easily

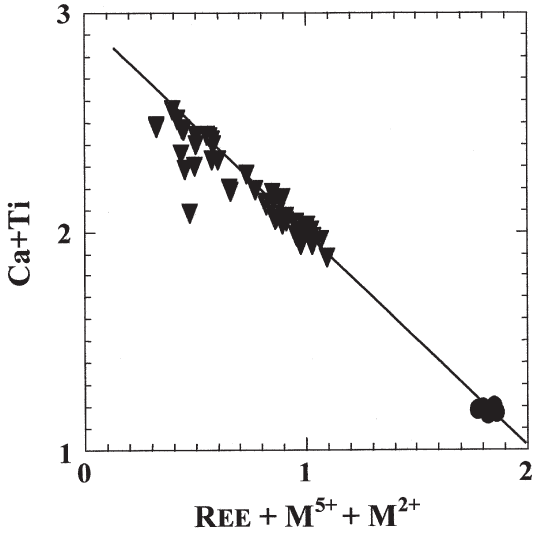

FIG. 3. Ca + Ti *versus REE* + M^{2+} + M^{5+} relationship for the Laacher See zirconolite. Filled dots: this work; filled triangles: metasomatic *REE*-rich zirconolite from Adamello and Bergell (data from Williams & Gieré 1996).

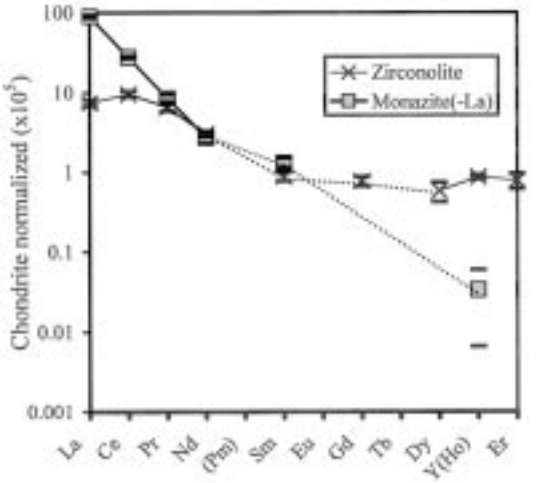

FIG. 4. Chondrite-normalized *REE* patterns of zirconolite and monazite-(La). Chondrite values from Wakita *et al.* (1971).

accommodate cations larger than Ca^{2+} (*i.e.*, $r > 0.112$ nm: Smith & Lumpkin 1993). Hence elements La^{3+} and Ce^{3+}, with ionic radii of 0.116 and 0.114 nm, respectively, as well as those cations that, in many mineral structures may substitute for Ca (*e.g.*, Sr, Ba, Pb), are largely excluded from the zirconolite structure. Thus the majority of terrestrial examples for which chondrite-normalized patterns have been obtained (*e.g.*, Fowler & Williams 1986, Platt *et al.* 1987, Bellatreccia *et al.* 1999) typically display a maximum at the position of Pr or Nd ($r = 0.113$ and 0.111 nm, respectively) even though crystallization may have involved a fluid relatively enriched in the lightest *REE* (the examples quoted are from carbonatites or nepheline syenites). Lunar zirconolite, and that occurring in fractionated magmas, have heavy-*REE* chondrite-normalized patterns that broadly reflect the chemical characteristics of the geological environment of crystallization (Gieré *et al.* 1998). Therefore, the chondrite-normalized pattern of zirconolite from Laacher See, with the maximum at Ce (Fig. 4), is unusual and must reflect crystallization from a fluid with a very enriched light-*REE* signature. It is noteworthy that the only other recorded example of zirconolite with a similar chondrite-normalized pattern is also from a syenite, that from Glen Dessarry, Scotland (Fowler & Williams 1986).

Monazite is a relatively common accessory mineral in granitic pegmatites, syenites and alkali-rich environments in general, as well as in carbonatitic rocks (Chang *et al.* 1996). It is generally enriched in *LREE* (*e.g.*, Fleischer & Altschuler 1969), commonly displaying steeply fractionated chondrite-normalized patterns (*e.g.*, Della Ventura *et al.* 1996). The chondrite-normalized pattern for the Laacher See monazite (Fig. 4) appears typically that of monazite from these parageneses, but it is significantly more enriched in La than most reported examples of monazite; the species is monazite-(La) and not the more typical monazite-(Ce). Thus both zirconolite and monazite-(La) are exceptionally enriched in the lightest *REE*, which suggests that they probably crystallized contemporaneously from the same fluid.

CONCLUSIONS

Basement xenoliths in the pyroclastic formations of the East Eifel volcanic field are well known, and have been studied since the last century (*e.g.*, Nöggerath 1824). According to Brauns (1911), these xenoliths represent regionally metamorphosed country-rocks that have a pronounced metasomatic overprint, *e.g.*, the sanidinites that show the effect of highly alkaline metasomatic fluids on regional metamorphic precursors (Frechen 1947, Wörner *et al.* 1982). Elements such as Ti, Zr, Nb and the *REE* can be very mobile in such environments (Michard 1989, Rubin *et al.* 1993, Gieré 1996). The late-stage volcanic activity in the Eifel region led to an enrichment in these elements, as documented by the abundance of rare minerals such as låvenite, wöhlerite, thorite, narsarsukite and pyrochlore-group minerals in the sanidinites (Hentschel 1983). The present study provides a further example of this phenomenon, with the recorded presence of *REE*, Nb-rich zirconolite and monazite-(La).

Acknowledgements

We are grateful for discussions with Drs. G.R. Lumpkin and K.L. Smith, and for detailed comments from referees P. Uher and E. Essene, and from R.F. Martin, that have helped clarify and improve significantly various aspects of this manuscript.

References

Bayliss, P., Mazzi, F., Munno, R. & White, T.J. (1989): Mineral nomenclature: zirconolite. *Mineral. Mag.* **53**, 565-569.

Bellatreccia, F., Della Ventura, G., Caprilli, E., Williams, C.T. & Parodi, G.C. (1999): Crystal chemistry of zirconolite and calzirtite from Jacupiranga, Saõ Paulo (Brazil). *Mineral. Mag.* **63**, 649-660.

Bogaard, P.V.D. & Schmincke, H.-U. (1984): The eruptive center of the late Quaternary Laacher See tephra. *Geol. Rundsch.* **73**, 933-980.

Borodin, L.S., Bykova, A.B., Kapitanova, T.A., & Pyatenko, Yu.A. (1960): New data on zirconolite and its niobium variety. *Dokl. Acad. Sci., Earth Sci. Sect.* **134**, 1022-1024.

Brauns, R. (1911): *Die kristallinen Shiefer des Laacher-See-Gebiets und ihre Umbildung zu Sanidinit.* E. Schweizerbart'sche Verlagsbuchhandlung, Stuttgart, Germany.

Brøgger, W.C. (1890): Die Mineralien der Syenitpegmatitgänge der Südnorwegischen Augit- und Nephelinsyenite. 46. Polymignyt. *Z. Krystall. Mineral.* **16**, 387-396.

Bulakh, A.G., Nesterov, A.R., Anisimov, I.S. & Williams, C.T. (1998): Zirkelite from the Sebl'yavr carbonatite complex, Kola Peninsula: an X-ray and electron microprobe study of a partially metamict mineral. *Mineral. Mag.* **62**, 837-846.

Chang, L.L.Y., Howie, R.A. & Zussman, J. (1996): *Rock-Forming Minerals.* 5B. *Non-Silicates: Sulphates, Carbonates, Phosphates, Halides* (2nd ed.). Longman Publishers, Harlow, U.K.

Coelho, A.A. (1995): *An X-Ray and Neutron Diffraction Investigation of Rare Earth Substituted Zirconolite Compounds.* Ph.D. thesis, Univ. of Technology, Sydney, Australia.

_____, Cheary, R.W. & Smith, K.L. (1997): Analysis and structural determination of Nd-substituted zirconolite-4M. *J. Solid State Chem.* **129**, 346-359.

Della Ventura, G., Mottana, A., Parodi, G.C., Raudsepp, M., Bellatreccia, F., Caprilli, E., Rossi, P. & Fiori, S. (1996): Monazite–huttonite solid-solutions from the Vico Volcanic Complex, Latium, Italy. *Mineral. Mag.* **60**, 751-758.

Droop, G.T.R. (1987): A general equation for estimating Fe^{3+} concentrations in ferromagnesian silicates and oxides from microprobe analyses, using stoichiometric criteria. *Mineral. Mag.* **51**, 431- 435.

Fielding, P.E. & White, T.J. (1987): Crystal chemical incorporation of high level waste species in aluminotitanate-based ceramics: valence, location, radiation damage, and hydrothermal durability. *J. Mater. Res.* **2**, 387-414.

Fleischer, M. & Altschuler, Z.S. (1969): The relationship of the rare earth composition of minerals to geological environment. *Geochim. Cosmochim. Acta* **33**, 725-732.

Fowler, M.B. & Williams, C.T. (1986): Zirconolite from the Glen Dessarry syenite: a comparison with other Scottish zirconolites. *Mineral. Mag.* **50**, 326-328.

Frechen, J. (1947): Vorgange der Sanidinitbildung im Laacher-See-Gebiet. *Fortschr. Mineral.* **26**, 147-166.

Gieré, R. (1986): Zirconolite, allanite and hoegbomite in a marble skarn from the Bergell contact aureole: implications for mobility of Ti, Zr and REE. *Contrib. Mineral. Petrol.* **93**, 459-470.

_____ (1990): Hydrothermal mobility of Ti, Zr and REE: examples from the Bergell and Adamello contact aureoles (Italy). *Terra Nova* **2**, 60-67.

_____ (1996): Formation of rare-earth minerals in hydrothermal systems. *In* Rare Earth Minerals, Chemistry, Origin and Ore Deposits (A.P. Jones, F. Wall & C.T. Williams, eds.). *Mineral. Soc., Ser.* **7**. Chapman and Hall, London, U.K. (105-150).

_____ & Williams, C.T. (1992): REE-bearing minerals in a Ti-rich vein from the Adamello contact aureole (Italy). *Contrib. Mineral. Petrol.* **112**, 83-100.

_____, _____ & Lumpkin, G.R. (1998): Chemical characteristics of natural zirconolite. *Schweiz. Mineral. Petrogr. Mitt.* **78**, 433-459.

Heaman, L.M. & LeCheminant, A.N. (1993): Paragenesis and U–Pb systematics of baddeleyite (ZrO_2). *Chem. Geol.* **110**, 95-126.

Hentschel, G. (1983): *Die Mineralien der Eifelvulkane.* Christian Weise Verlag, Munich, Germany.

Kesson, S.E., Sinclair, W.J. & Ringwood, A.E. (1983): Solid solution limits in SYNROC zirconolite. *Nucl. Chem. Waste Manag.* **4**, 259-265.

Larsen, A.O. (1996): Rare earth minerals from the syenite pegmatites in the Oslo region, Norway. *In* Rare Earth Minerals: Chemistry, Origin and Ore Deposits (A.P. Jones, F. Wall & C.T. Williams, eds.). *Mineral. Soc. Ser.* 7. Chapman and Hall, London, U.K. (151-166).

LUMPKIN, G.R., SMITH, K.L. & GIERÉ, R. (1997): Application of analytical electron microscopy to the study of radiation damage in the complex oxide mineral zirconolite. *Micron* **28**, 57-68.

MAZZI, F. & MUNNO, R. (1983): Calciobetafite (new mineral from the pyrochlore group) and related minerals from Campi Flegrei, Italy: crystal structures of polymignyte and zirkelite: comparison with pyrochlore and zirconolite. *Am. Mineral.* **68**, 262-276.

MICHARD, A. (1989): Rare earth element systematics in hydrothermal fluids. *Geochim. Cosmochim. Acta* **53**, 745-750.

NÖGGERATH, J. (1824): *Das Gebirge in Rheinland-Westphalen* **3**. Eduard Weber Verlag, Bonn, Germany.

PLATT, R.G., WALL, F., WILLIAMS, C.T. & WOOLLEY, A.R. (1987): Zirconolite, chevkinite and other rare minerals from nepheline syenites and peralkaline granites and syenites of the Chilwa alkaline province, Malawi. *Mineral. Mag.* **51**, 253-263.

RUBIN, J.N., HENRY, C.D., & PRICE, J.G. (1993): The mobility of zirconium and other "immobile" elements during hydrothermal alteration. *Chem. Geol.* **110**, 29-47.

SHANNON, R.D. (1976): Revised effective ionic radii and systematic studies of interatomic distances in halides and chalcogenides. *Acta Crystallogr.* **A32**, 751-767.

SILVA, L.C. & FIGUEIREDO, M.O. (1980): Note on the occurrence of niobium-rich zirconolite in carbonatitic rocks of Santiago island (Cape Verde Republic). *Garcia de Orta, Ser. Geol.* **4**(1-2), 1-6.

SINCLAIR, W. & EGGLETON, R.A. (1982): Structure refinement of zirkelite from Kaiserstuhl, West Germany. *Am. Mineral.* **67**, 615-620.

_____ & RINGWOOD, A.E. (1981): Alpha-recoil damage in natural zirconolite and perovskite. *Geochem. J.* **15**, 229-243.

SMITH, K.L. & LUMPKIN, G.R. (1993): Structural features of zirconolite, hollandite and perovskite, the major waste-bearing phases in Synroc. *In* Defects and Processes in the Solid State: Geosciences Applications (J.N. Boland & J.D. Fitz-Gerald, eds.). Elsevier, New York (401-422).

WAKITA, H., REY, P. & SCHMITT, R.A. (1971): Abundances of the 14 rare-earth-elements and 12 other trace elements in Apollo 12 samples: five igneous and breccia rocks and four soils. *Proc. 2nd Second Lunar Sci. Conf., Geochim. Cosmochim. Acta, Suppl.* **2**(2), 1319-1329.

WHITE, T.J. (1984): The microstructure and microchemistry of synthetic zirconolite, zirkelite and related phases. *Am. Mineral.* **69**, 1156-1172.

WILLIAMS, C.T. (1996): Analysis of rare earth minerals. *In* Rare Earth Minerals: Chemistry, Origin and Ore Deposits (A.P. Jones, F. Wall & C.T. Williams, eds.). *Mineral. Soc., Ser.* **7**. Chapman and Hall, London, U.K. (327-348).

_____ & GIERÉ, R. (1988): Metasomatic zonation of REE in zirconolite from a marble skarn at the Bergell contact aureole (Switzerland/Italy). *Schweiz. Mineral. Petrol. Mitt.* **68**, 133-140.

_____ & _____ (1996): Zirconolite: a review of localities worldwide, and a compilation of its chemical composition. *Nat. Hist. Mus. London, Bull.* **52**, 1-24.

WÖRNER, G., SCHMINCKE, H.-U. & SCHREYER, W. (1982): Crustal xenoliths from the Quaternary Werh volcano (East Eifel). *Neues Jahrb. Mineral., Abh.* **144**, 29-55.

ZAKRZEWSKI, M.A. LUSTENHOUWER, W.J., NUGTEREN, H.J. & WILLIAMS C.T. (1992): Rare-earth minerals yttrian zirconolite and allanite-(Ce) and associated minerals from Koberg mine, Bergslagen, Sweden. *Mineral. Mag.* **56**, 27-35.

Received April 22, 1999, revised manuscript accepted January 25, 2000.